

CNRS
Centre National de la Recherche Scientifique

INFN
Istituto Nazionale di Fisica Nucleare



**The VIRGO north arm cavity:
Examples for the use of the interferometer simulation
FINESSE**

VIR-NOT-EGO-1390-269

A. Freise, M.Loupias

Issue: 1

Date: 16th June 2004

VIRGO * A joint CNRS-INFN Project
Via E. Amaldi, I-56021 S. Stefano a Macerata - Cascina (Pisa)
Secretariat: Telephone (39) 050 752 521 * FAX (39) 050 752 550 * Email W3@virgo.infn.it

Contents

1	Introduction	1
2	Setting up the optical components	2
3	Tuning the simulation using measured data	3
4	Modulation-demodulation	6
4.1	Mode-separation frequency	7
4.2	Modulation frequency for the liner alignment	9
5	The injection bench	11
5.1	Beam size and shape	14
6	Linear alignment	17
7	Conclusion	20

1 Introduction

The north arm cavity of the gravitational-wave detector VIRGO [1] has been installed and commissioned in 2003 and 2004. It is a 3 km long Fabry-Perot cavity consisting of a flat input mirror and a spherically curved end mirror. Such a cavity represents a very simple optical system. Nevertheless, it provides some challenges, because of the extreme sensitivity required for the gravitational-wave detector.

After the basic installation of the optics, the cavity had to be characterized, control systems were to be implemented and the performance of the system optimized. All these tasks use well-known techniques which are not explained in this document. However, during this work an optical simulation represents a useful tool. Several simulations with FINESSE [2] have been done during the work on the north arm cavity. Step by step, the FINESSE input file describing the optical setup has been tuned, i. e. several parameters have been updated according to measurement results. During this process the simulation results helped to characterize the experimental setup and also helped in understanding unforeseen behavior of the optical setup.

The aim of this document is to describe and document the obtained results from the comparisons of the simulation with the data, for example, optical parameters like the finesse of the cavity. At the same time it is meant as a introduction to optical simulations, especially to the FINESSE program. An optical simulation sometimes turns out to require a similar effort as the experimental work on the respective optical setup; a lot of care and experience is necessary to create correct and meaningful data. The descriptions of the FINESSE input files below should provide some information on how the mentioned simulation results were obtained.

The Finesse input files

FINESSE is not an interactive program; the program reads an input file, performs the requested computation, saves the output data in another text file and calls Gnuplot to create a plot from that data. The input file must contains a description of the optical setup and the commands specifying the simulation task. Throughout this document excerpts of the input files are shown and the names of the input files are noted. These files can currently be found on a webpage [3].

The simulations were performed using FINESSE 0.97 but most input files are simple and can also be used with older versions of the program.

2 Setting up the optical components

Figure 1 shows a very simple sketch of the north arm cavity of VIRGO. The cavity is formed by a flat (NI) and a spherical mirror (NE). The input light is coupled into the cavity via NI. NE is high reflective so that the cavity is over-coupled. The cavity length is approximately 3 km.

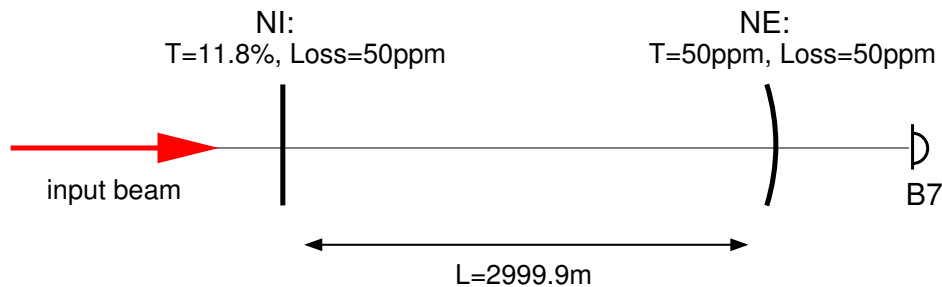


Figure 1: Simplified setup of the north arm cavity: the north input mirror (NI) and the north end mirror (NE) form a linear Fabry-Perot cavity. The transmitted light is detected by a photo diode (B7).

The first step with FINESSE is to create a similarly simplified input file with the parameters of the mirrors. For the moment we restrict the analysis to plane waves. Hence, parameters that describe off-axis properties, like the radii of curvatures, can be omitted (`00first.kat`):

```
l i1 1 0 0 nin          # dummy input light: 1W
s sNs 6 nin nMNI1      # arbitrary distance to NI
# North Input Mirror T=11.6%, Loss=50ppm
m MNI 0.88195 0.118 0 nMNI1 nMNI2
s sNl 2999.9 nMNI2 nMNE1 # cavity length
# North End Mirror T=50ppm, Loss=50ppm
m MNE 0.9999 50u 0 nMNE1 noutB7
```

In addition to the two mirrors, a dummy input laser is specified. The values for the transmission and reflection of the mirrors correspond to the specifications. The 50 ppm losses are typical numbers for high quality optical surfaces in similar setups. The distance between the two mirrors has been derived from geodetic position measurements.

A sensible first step is to check the operating point of the system. The operating point is the equilibrium state of the system (with or without active controls). Usually, it makes sense to represent the operating point by the component parameters in the FINESSE input file. In this case the input light should be resonant in the cavity. To check this, we move NE away from its nominal position and plot the power transmitted by the cavity (`00first.kat`):

```
pd B7 noutB7          # light power transmitted by the cavity
xaxis MNE phi lin -20 20 300 # tuning MNE from -20 to 20 degrees
```

In FINESSE moving a mirror longitudinally on a microscopic scale is called *tuning* the mirror: the parameter `phi` gives the displacement of the mirror from the nominal position in degrees whit 360° corresponding to one wavelength. For example, in order to change the operating point of the cavity from longitudinal resonance to the next, one has to move one mirror by $\lambda/2$, i. e. 180° .

The output of the simulation is shown in Figure 2: the resonance of the cavity is located as expected at the operating point ($\phi_{NE} = 0$).

As a next step the cavity parameters can be checked. To compute the cavity parameters we can at this point already specify the curvature of the end mirror and thus switch to an analysis using Hermite-Gauss modes (`01cavity-mode.kat`):

```
attr MNE Rc 3600      # radius of curvature of NE
```

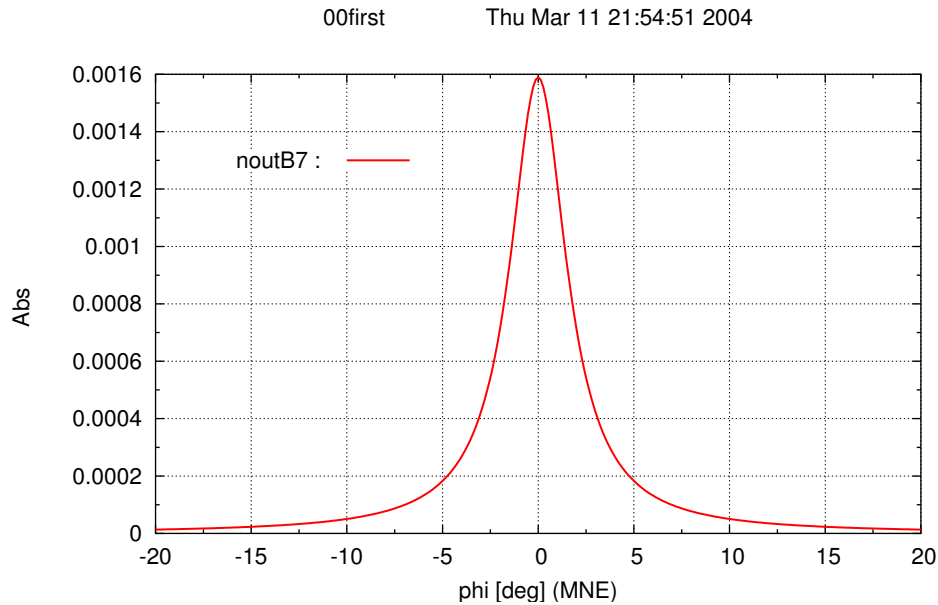


Figure 2: Light power transmitted by the cavity as a function of the microscopic position (*tuning*) of the north end mirror. The operating point is at the resonance for $\phi = 0$ deg. (00first.kat)

```
cav NC MNI nMNI2 MNE nMNE1 # compute cavity
maxtem 0 # order of higher order modes (n+m)
trace 2 # print cavity parameters
```

The radius of curvature of the mirror has been measured to be $R_C = 3580$ m at 150 mm diameter and $R_C = 3625$ at 280 mm diameter (with a coating diameter of 330 mm). For the simulation the mean of these two numbers is used.

With the otherwise unchanged file we can produce exactly the same plot as in Figure 2 and in addition, the command `trace 2` causes FINESSE to print the cavity parameters:

```
--- cavity tracing
cavity NC:
cavity is stable! Eigenvalues:
q=1341.73i, w0=21.317117mm z=0m
Finesse : 49.96, Round-trip loss: 0.118138195
opt. length: 5.9998km, FSR: 49.967075kHz, FWHM: 1.0001179kHz
```

3 Tuning the simulation using measured data

Measured data from the VIRGO north arm cavity can be used to *tune* the simulation, i. e. to adapt certain parameters in the input file in order to match the simulation results to measurements.

In the following examples the higher order transverse modes will play a role. In such a case it is important to introduce the secondary surfaces of the mirrors and beam splitter to the input file. A main mirror in a interferometric gravitational wave detector typically has one high reflective surface whereas the secondary surface is coated for anti-reflection. Fused silica is often used as a substrate material. Such a mirror can be modeled in FINESSE by using 3 components file: 02fringes.kat:

```
m MNE 0.9999 50u 0 nMNE1 nMNEi1 # primary surface
s sMNE .096 1.44963 nMNEi1 nMNEi2 # fused silica substrate
m MNEAR 0 1 0 nMNEi2 nMNE2 # secondary surface (AR coated)
```

This example shows how the north end mirror can be composed of two mirror components and a space component. The name of the component ‘mirror’ is slightly misleading since it is only a partly reflecting surface under normal incidence. In the same sense the beam splitter component is a partly reflecting surface for arbitrary incidence. The north end mirror primary surface is high reflective, the fused silica substrate is 9.6 cm thick and the secondary surface is coated for anti-reflection. Actually, the currently installed NE mirror has no coating on the secondary surface. But for the next steps in this simulation task we can ignore the properties of the secondary surface (but not its existence and the substrate).

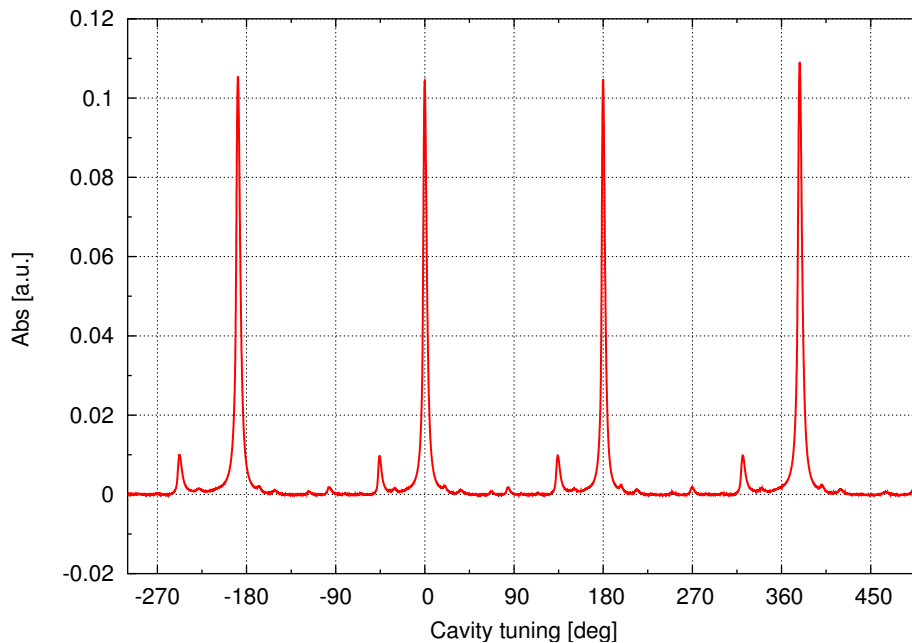


Figure 3: The measured power transmitted by the north arm cavity (detected by photo diode B7). The data was taken when the cavity was not longitudinally locked and the mirrors were aligned very well. The data shows the resonance peaks as a function of time. The x-axis has been rescaled assuming a linear differential mirror motion of 5λ per second. In FINESSE the mirror motion is expressed in degrees with 360° representing a change in position of λ . The x-axis has thus been put in degrees and labeled ‘cavity tuning’. The distance between two large peaks, i. e. one free spectral range, represents a length change of $\lambda/2$ (180°). The time between two large peaks is 0.1 sec. It can be seen that the fringes are almost equally spaced which indicates that the cavity tuning can be simulated by a linear change of the cavity length.

The first useful set of data is the transmitted power of the cavity while the cavity mirrors were longitudinally uncontrolled. Figure 3 shows such a data stretch. The large peaks correspond to a main resonance, i. e. at those times the TEM_{00} of the laser light is resonant in the cavity. In FINESSE the resonance of the cavity is changed by tuning a mirror. To move from one resonance of the TEM_{00} to the next of a TEM_{00} one has to change the position of one mirror by $\lambda/2$, i. e. to tune one mirror by 180° . In Figure 3 the x-axis has been rescaled accordingly.

These resonance peaks of an uncontrolled cavity are also called *fringes*. These fringes can be used to measure, for example, the round trip loss of a cavity. Figure 4 shows again the same data, but in a different way. First of all, three successive stretches of data have been superimposed. In addition, the y-scale has been changed so that the resonance peaks of higher order spatial modes can be seen more clearly. This plot is helpful to check the linearity of the longitudinal motion of the mirrors: It can be seen that the distance (in time) between two main resonance peaks and also the distance between the main peaks and those of higher order modes are roughly the same. This means that a simulation that uses a linear motion of one mirror should be able to reproduce the measured data.

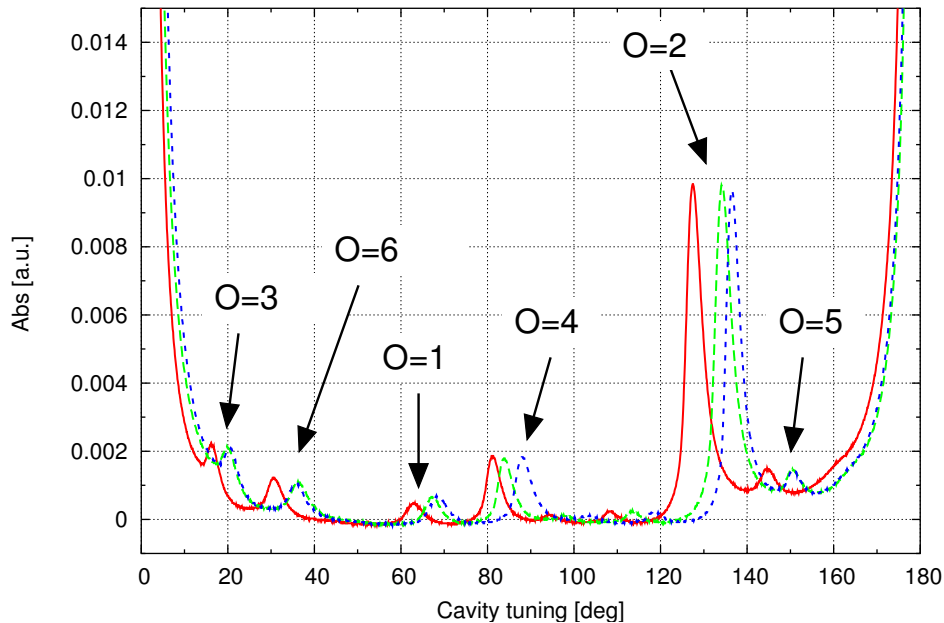


Figure 4: This plot shows the same measured data as Figure 4 but is this plot three successive stretches of data representing each one free spectral range have been superimposed in order to check the linearity of the cavity length change. A different y-scale has been chosen to better show the resonances of higher order modes. The labels give the order ($n+m$) of a TEM_{nm} mode that creates the respective peak. It can be seen that the second order modes are dominant while also modes up to the 6th order are visible.

A FINESSE simulation to plot a set of similar fringes can be performed using the following commands (02fringes.kat):

```
pd B7 nMNE2
xaxis MNI phi lin -100 300 2000
```

The first parameter to adjust in the simulation will be the round-trip loss of the cavity and hence its finesse. Another parameter that can and should be tuned by looking at the transmitted power is the curvature of the north end mirror, now set to 3600 m.

The input file for FINESSE still misses some parameters for reproducing the peaks for higher order modes. The dominant imperfections will be a non-perfect alignment of the cavity mirrors and a mode-mismatch of the input beam to the cavity. In order to add such defects to the simulation one uses the commands `gauss`, for setting a mode-mismatch, and `attr` for misaligning the mirrors (02fringes.kat):

```
gauss g1 MNIAR nMNI1 12.8m -4 # creating a mode mismatch
attr MNI ybeta 1u # some arbitrary mis-alignment
attr MNE xbeta -.3u # some arbitrary mis-alignment
```

The first line, i.e. the `gauss` command, causes FINESSE to set the user-defined beam parameter¹, here $w = 14.8$ mm and $z = -4$ m, at the outer node of the north input mirror whereas the beam parameter *inside* the cavity is still being derived from the eigen-mode. This enforces a mode-mismatch at the north input mirror.

The two lines with `attr` are used to set typical values for the mis-alignment of the cavity mirror, assuming that the mirrors were carefully aligned manually.

The output of the simulation is shown, superimposed with the measured data, in the three plots: In Figure 5 the output of the tuned simulation and the measured data is plotted. Figure 6 and Figure 7 show zooms into

¹ the beam parameters shown here represent already the result of a manual tuning of the simulation

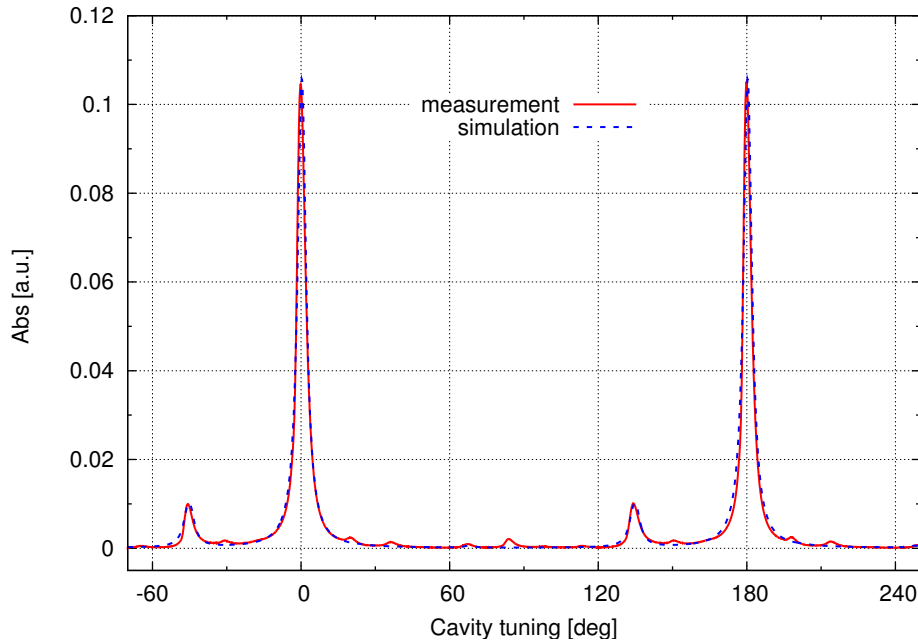


Figure 5: Comparison of simulated with measured data for the light transmitted by the north cavity. The simulation has been tuned so that the resonances of the TEM_{00} and the peaks associated with $n + m = 2$ are well matched. (02fringes.kat)

the same data. Figure 6 zooms in onto one resonance of the TEM_{00} : a perfect agreement of the simulation with the measurement cannot be achieved with a static simulation. However, by carefully adjusting the reflection of the NI mirror, the best match was achieved for a NI reflection of $R = 0.864$. Compared to the nominal value, this indicates an extra round-trip loss of approximately 1.8% or respective a higher transmission of the cavity mirrors. The choice of lowering the NI reflectivity was arbitrary (02fringes.kat):

```
#m MNI 0.88195 0.118 0 nMNIi2 nMNI2 # primary surface
# above: untuned, below tuned: adding 1.8% more losses -> Finesse = 43
m MNI 0.864 0.118 0 nMNIi2 nMNI2
```

In order to understand whether extra losses or a deviation of the mirror parameters are present one has to tune simultaneously the data for the reflected and the transmitted power. This is still to be done.

Finally, Figure 7 shows that the distance between the resonance peaks for $n + m = 0$ and $n + m = 2$ can be matched by changing the radius of curvature of the NE mirror to $ROC_{NE} = 3530$ m. The same result could be achieved by increasing the cavity length by 62 m but the cavity length had been measured accurately whereas the curvature of a mirror typically is known with some uncertainty.

4 Modulation-demodulation

The control systems used for stabilizing the longitudinal and angular degrees of freedom of the mirrors make use of modulation-demodulation techniques: the laser light is modulated in phase at a fixed frequency f_{mod} (the *modulation frequency*, usually at several MHz) before it enters the interferometer. The control signals are derived by demodulating the photo diode signal at this modulation frequency.

Figure 14 shows a schematic of the components located on an optical table behind the north end mirror. The photo diodes on this so-called *north external bench* can be used to obtain signals for the longitudinal and the

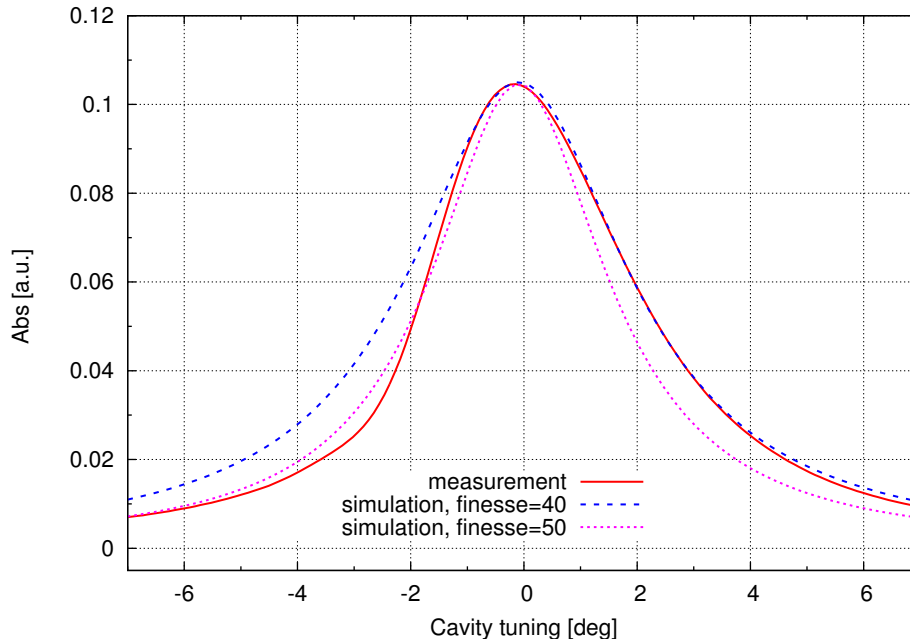


Figure 6: Comparison of simulation with measured data for the light transmitted by the north cavity. The resonance of the TEM_{00} mode can be tuned to have a similar shape by adding extra losses to the north cavity. Please note that the measured peak is not symmetric. This shows that it can only be reproduced exactly by a dynamic simulation. The data produced by FINESSE (a static simulation) cannot be matched well. But it can be seen that the finesse will be between 40 and 50. In the following, an extra round-trip loss of 1.8% has been used. This yields a finesse of 43 and seemed to fit best to the measurements.

angular control of the cavity mirrors. In both cases a phase modulation of the laser light at $f_{\text{mod}} \approx 6$ MHz is performed. The longitudinal signal is obtained by demodulating the signal of B7 at f_{mod} . For the alignment control split photo diodes, so-called *quadrant diodes* (QD) are used. They are composed of four separate elements. To obtain, for example, error signals for the horizontal alignments of the mirrors, the difference between the signals from the left and right quadrant is computed and this signal is then demodulated at f_{mod} . This technique is called *differential wave-front sensing*, and in the special case when the signal is generated in transmission of the cavity (as described here) this is the Anderson technique [7].

4.1 Mode-separation frequency

The Anderson technique requires a phase modulation of the input light at a specific frequency which is has to be a resonance frequency of the TEM_{01} mode. Thus:

$$f_{\text{mod}} = N \text{FSR} + f_{\text{sep}} \quad (1)$$

with N as a integral number, FSR the free spectral range of the cavity and f_{sep} as the so-called mode separation frequency, which is the difference between the resonance frequencies of TEM modes for different mode numbers:

$$f_{\text{sep}} = f_{n+1,m} - f_{n,m} = \frac{\Psi_{\text{rt}} c}{2\pi l} \quad (2)$$

with $f_{n,m}$ as the resonance frequency of a TEM_{nm} mode, c , the speed of light, l the round trip length and Ψ_{rt} the round trip Gouy phase.

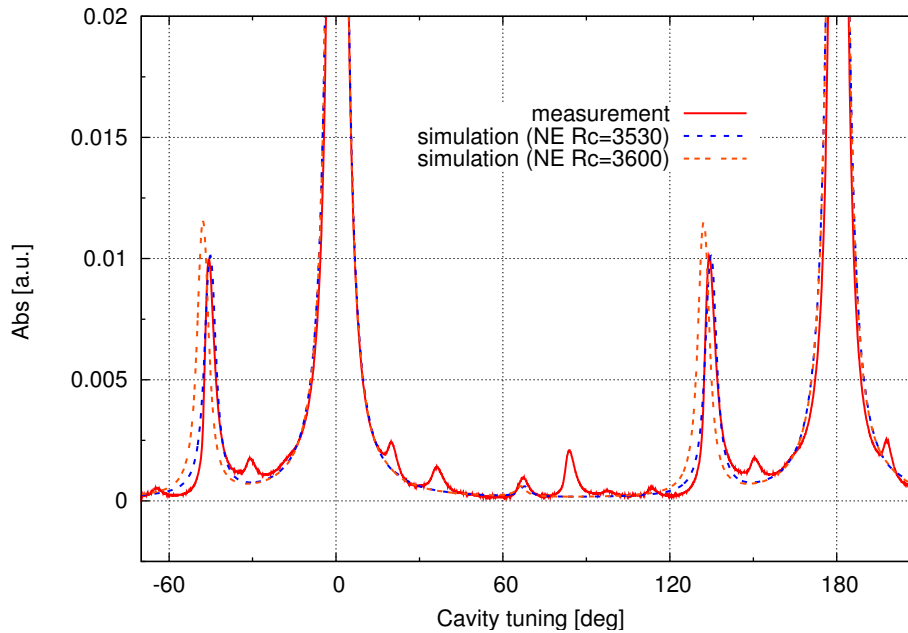


Figure 7: Comparison of simulated with measured data for the light transmitted by the north cavity. The plot shows traces of simulated data for two different values for the radius of curvature of the NE mirror. It can be seen that a distance between the two resonance peaks can be matched by changing the value from the nominal 3600 m to 3530 m.

FINESSE can be used in two ways to help in finding the mode-separation frequency. The first method is to get the Gouy phase by running the file `03mode-separation.kat` again using this time the command `trace 18`. This yields an extra output:

```
--- setting Gouy phase for all spaces:
...
space sN1: gouy_x=1.172859rad=67.199868deg, gouy_y=1.172859rad=67.199868deg
```

The round trip Gouy phase is given as:

$$\Psi_{rt} = 2 \times 1.172859 \approx 2.35 \quad (3)$$

And thus we get:

$$f_{sep} = \frac{\Psi_{rt} c}{2\pi l} \approx \frac{2.3 \cdot 3^8}{2\pi \cdot 6000} \approx 18.7 \text{ kHz} \quad (4)$$

A second method is to plot the resonances of several higher order modes. For example, the input light can be setup so that the power is equally distributed into 6 TEM modes (`03mode-separation.kat`):

```
tem i1 0 0 1 0      # dividing the input power
tem i1 0 1 1 0      # equally to 6 modes:
tem i1 0 2 1 0      # TEM_00 to TEM_05
tem i1 0 3 1 0
tem i1 0 4 1 0
tem i1 0 5 1 0
```

Then the amplitude of light field transmitted by the cavity is detected with the ‘amplitude detector’ which allows to select the frequency and mode number:

```
ad ad0 0 0 0 noutB7      # detecting the anplitude
```

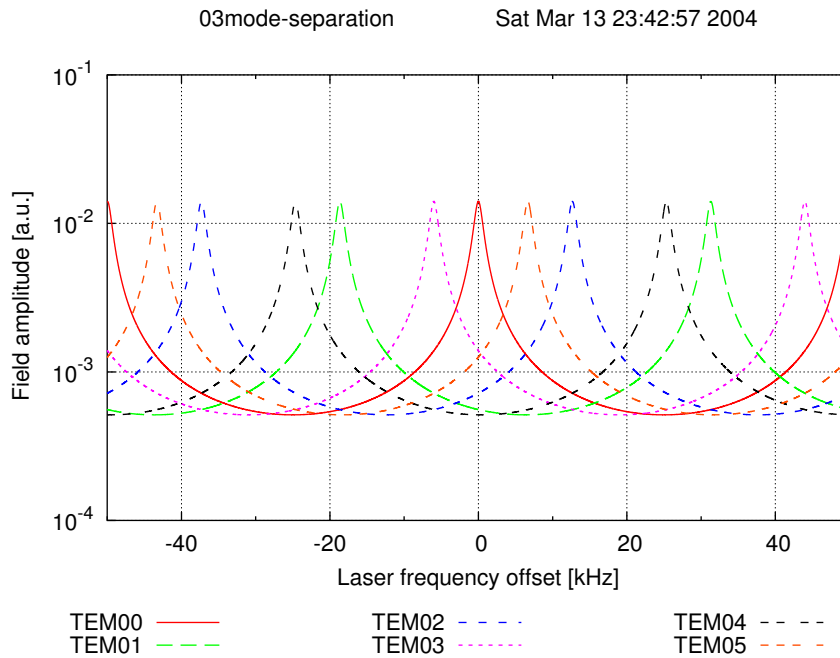


Figure 8: The resonances of several TEM fields in the north arm cavity as a function of the input light frequency (given as an offset to the default frequency). The frequency difference between the TEM_{nm} and the $TEM_{n,m+1}$, also called mode separation, is approximately 18.7 kHz. (03mode-separation.kat)

```
ad ad1 0 1 0 noutB7          # of TEM_00, TEM_01, ...
ad ad2 0 2 0 noutB7          # in transmission of the
ad ad3 0 3 0 noutB7          # cavity
ad ad4 0 4 0 noutB7
ad ad5 0 5 0 noutB7
```

To plot the resonances as a function of frequency, we sweep the laser (input light) frequency about plus/minus one free spectral range. Due to the nature of the amplitude detector, the frequency parameter of those has to be tuned explicitly too:

```
xaxis i1 f lin -50k 50k 10000 # tuning the laser frequency plus/minus
                                # 50 kHz around the default frequency

xparam ad0 f 1 0                # the amplitude detectors only "see" light
xparam ad1 f 1 0                # at one single frequency. So in order
xparam ad2 f 1 0                # to get a signal, we have to sweep the
xparam ad3 f 1 0                # frequency parameter of all detectors
xparam ad4 f 1 0                # with the laser frequency
xparam ad5 f 1 0
```

The resulting plot, shown in Figure 8, shows also the mode separation of ≈ 18.7 kHz.

4.2 Modulation frequency for the liner alignment

From the following section we see that one of the optimal modulation frequencies should be (using the numbers obtained in Section 2 for FSR and in Section 4.1 for f_{sep}):

$$f_{mod} = N \text{ FSR} + f_{sep} = 125 \times 49.967075 \text{ kHz} + 18.7 \text{ kHz} = 6.264584 \text{ MHz} \quad (5)$$

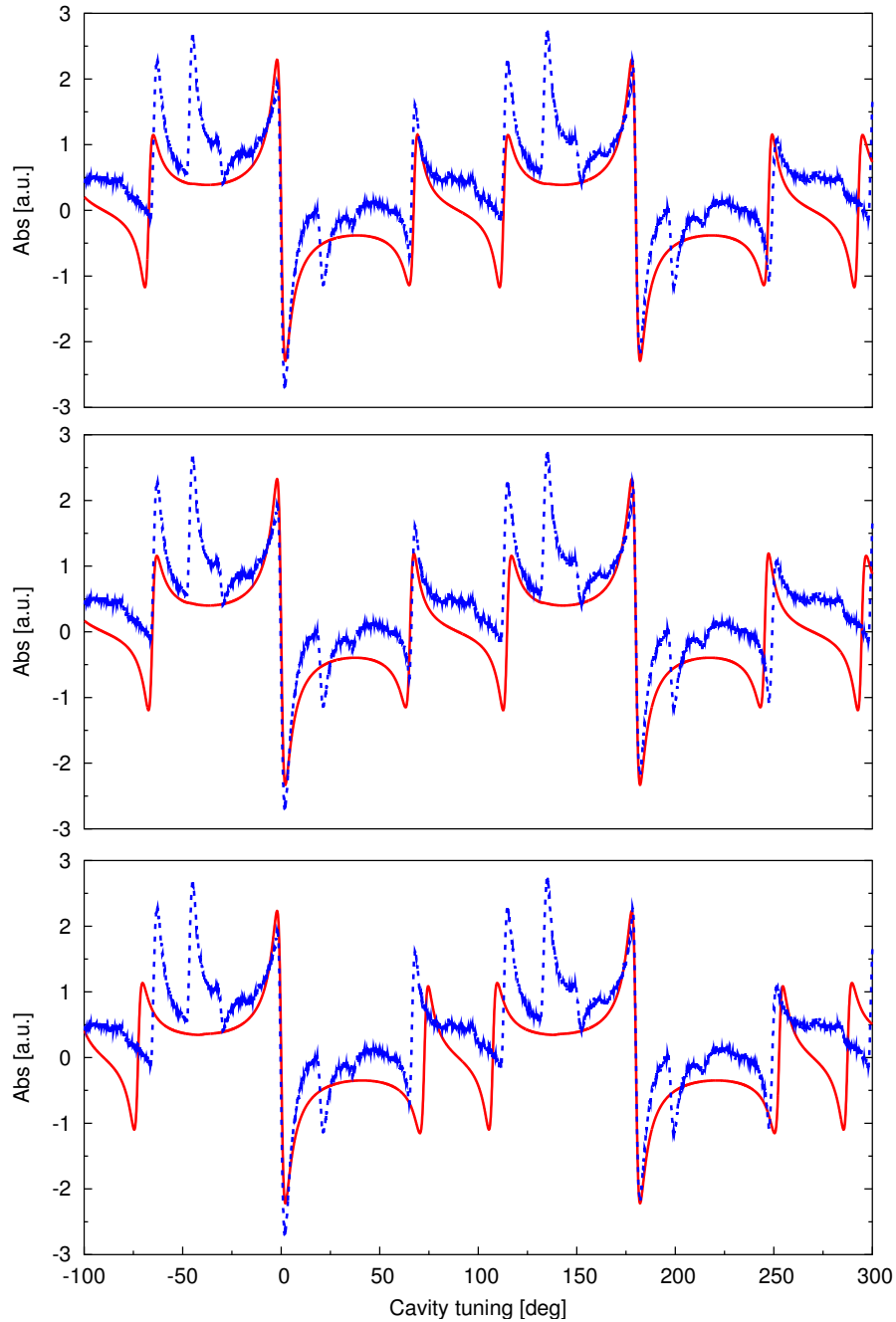


Figure 9: Simulation and measured data demodulated light power transmitted by the cavity, i. e. the AC output of B7 on the north bench. The simulation uses a demodulation phase of 30° (the experimental demodulation phase was unknown at the time the data was taken). The three graphs show the comparison between the measurement and the data for three different modulation frequencies: top: nominal frequency (6.264580 MHz), middle: the frequency currently used in the experiment (6.264080 MHz) and bottom: nominal frequency plus 2 kHz. (04modulation)

Currently used in the experiment is 6.264080 MHz. It seems that this frequency is approximately 500 Hz detuned from an optimum value, which would be just at the end of the range for tolerable mis-tuning.

A second set of simulations can be done to check the modulation frequency. Again, the output of the simulation is to be compared to measured data, this time the demodulated signal of the diode B7.

This file(s) `04modulation` are used to compute the demodulated signal of light power transmitted by the cavity for different modulation frequencies. The modulation is performed with a modulator after the input light:

```
#var fMI 6.264080M          # modulation frequency currently used
var fMI 6.264580M          # modulation frequency optimised for simulation
#var fMI 6.266080M          # modulation frequency currently used +2kHz

l i1 1 0 0 nin             # dummy input light: 1W
s sE0 1m nin nE01
mod eom1 $fMI .1 1 pm 0 nE01 nE02 # phase modulation
```

The demodulated signals are computed using a `pd` detector with one demodulation frequency:

```
#pd1 B70 $fMI 0 noutB7
pd1 B730 $fMI 30 noutB7
#pd1 B760 $fMI 60 noutB7
#pd1 B7DC90 $fMI 90 noutB7
```

The optimum demodulation phase of 30° has been found by comparing the error signals for various demodulation phase first (the signal with the steepest slope at the operating point, i. e. zero tuning, has been chosen).

The result for 30° is then compared to measured data, see Figure 9. The measured data was taken during the same period as the DC signal before.

Only the first order TEM modes have been used in the simulation. Therefore only some of the structures of the measured data can be reproduced, mainly the resonances of the TEM_{00} at 0° and 180° and the resonances of the sidebands, e.g. at approximately 60° and 110° . The comparison is not accurate enough to clearly state that the simulation using the value of the experimentally frequency fits better to the data than the simulation output using the computed optimum frequency that is 500 Hz detuned. But a detuning of 2 kHz clearly yields a mismatch between the measurement and the simulation, as depicted in the lowest plot.

5 The injection bench

The injection bench (IB) is a small optical bench suspended in vacuum. It supports several optical components used for injecting the beam from the laser to the input mode cleaner (IMC) and afterwards into the main interferometer (ITF). The optical setup of this bench is shown in Figure 10. The mode matching of the beam from the input mode cleaner into the arm cavities is done by three optical components: `M_LIB5`, `M_LIB6` and the power-recycling mirror. `M_LIB5` and `M_LIB6` are spherical mirrors that transform the beam parameter upon reflection. In addition, the substrate of the power-recycling mirror is used as a lens (the secondary surface is spherically curved). In order to adjust the mode matching `M_LIB6` can be translated by using motors.

For many simulations it makes little difference how the beam is matched to the arm cavity, but nevertheless it is worth adding the injection bench components to the file. First it allows to check if, for example, an astigmatism of the input beam creates an asymmetry between the signals for horizontal and vertical mirror alignment. And second, it is always worth while completing the input file as much as possible so that it is available and prepared for other simulation tasks.

In the file `05IB.kat` the components from the injection bench were added, starting at the output mirror of the IMC, using the parameters from OptoCad (a mixture of parameters from the design of the input bench and measured values):

```
l i1 6 0 0 nin
gauss g1 i1 nin 5e-3 -42.836m # nominal value
```

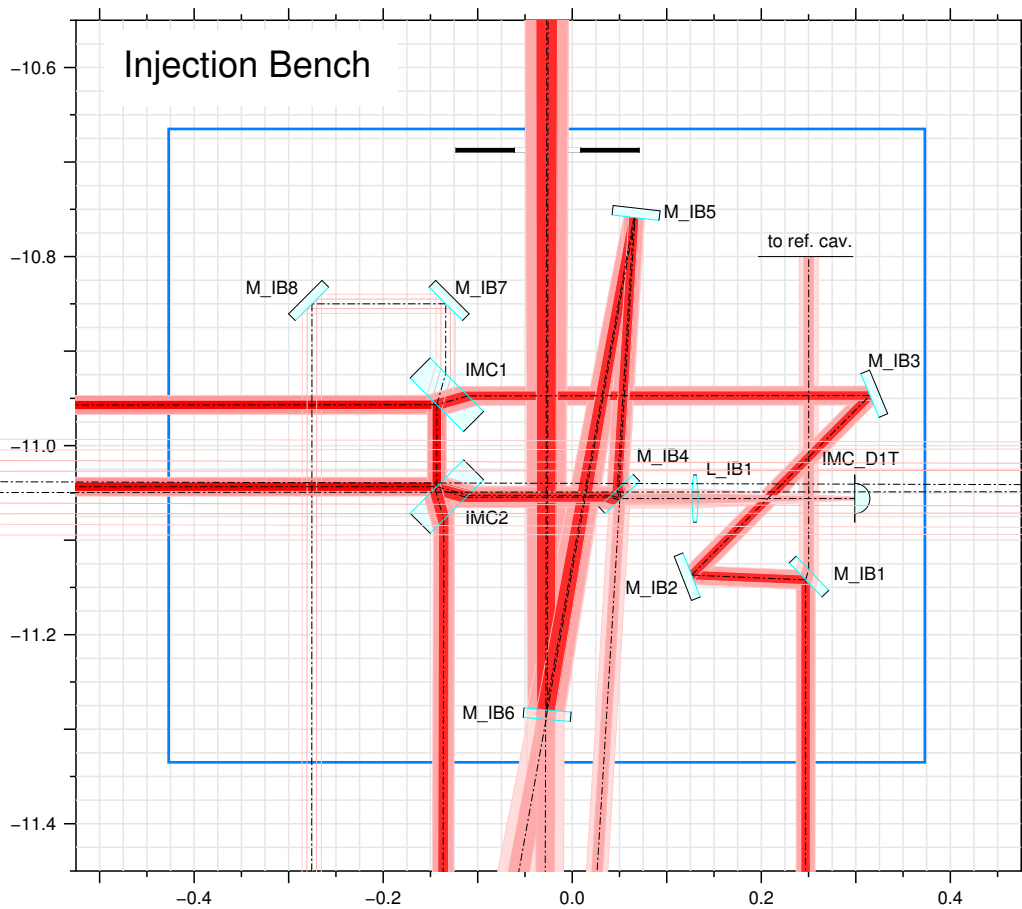


Figure 10: Optical layout of the injection bench. The plot has been created with Optocad [4]. The schematic shows several beams in connection with the IMC. For the moment we are only interested in the output beam of the IMC: IMC1 and IMC2 represent two mirrors of the triangular input mode cleaner cavity. The output beam leaves IMC2 towards M_IB4. M_IB5 and M_IB6 are spherical mirrors; they form a telescope (together with the power-recycling mirror, whose substrate serves as a lens) for matching the beam to the eigen-mode of the arm cavities. This mode-matching telescope can be adjusted by translating M_IB6 with motors.

```
# output mirror of IMC
bs IMC2i 0 1 0 -45.0 nin dump nIMC2i1 dump
s sIMC2 0.034 1.44963 nIMC2i1 nIMC2I2
bs IMC2o 0 1 0 -29.20 nIMC2I2 dump nIMC2o1 dump

# modulator for simplicity after IMC
s s0 1m nIMC2o1 nE01
mod eom1 $fMI .1 1 pm 0 nE01 nE02

s sM4 0.151 1 nE02 nM4a # distance from OptoCad
# mirror M_IB4 is currently mounted in reverse, so that the AR
# coating is in front and the beam passes the substrate twice.
bs M_IB4AR1 0 1 0 -46.71 nM4a dump nM4i1 dump
s sM41 12m 1.44963 nM4i1 nM4i2
bs M_IB4HR 0.999 0.001 0 -30.15 nM4i2 nM4i3 dump dump
s sM42 12m 1.44963 nM4i3 nM4i4
```

```

bs M_IB4AR2 0 1 0 30.14 nM4i4 dump nM4b dump
s s1 0.286 nM4b nM51 # distance from OptoCad

# mode matching telescope on IB
# angle of incidence on M_IB5 from OptoCad -3.3 deg
bs M_IB5 1 0 0 -3.3 nM51 nM52 dump dump
attr M_IB5 Rc -1.22
s s2 0.545 nM52 nM61 # distance measured
# angle of incidence on M_IB6 from OptoCad 5.0 deg
bs M_IB6 1 0 0 5 nM61 nM62 dump dump
attr M_IB6 Rc 3.16

s s3 .596 nM62 nD1
m Dia 0 1 0 nD1 nD2 # diaphragm (i.e aperture)
s s3b 4.68 nD2 nMPR1 # distance M_IB6-MPR (s3+s3b) is is 5.276

```

In this file a dummy input light is positioned just before the substrate of the output coupler of the IMC (IMC2). The beam parameter is set according to the optical design of the IMC (i.e. the waist position is between the two flat mirrors and the waist size is 5 mm).

The beam passes the substrate of IMC2, then is passing through the mode matching telescope consisting of M_IB5, M_IB6 and the substrate of MPR. At the time of writing (May 2004) the turning mirror M_IB4 is mounted in reverse so that the rear surface is actually the primary one so that the beam passes the substrate of M_IB4 twice.

The angles of incidence for the curved mirrors (M_IB5 and M_IB6) are important for computing the astigmatism of the beam. The numbers have been computed with OPTOCAD. The several substrates are also included in order to compute the astigmatism properly.

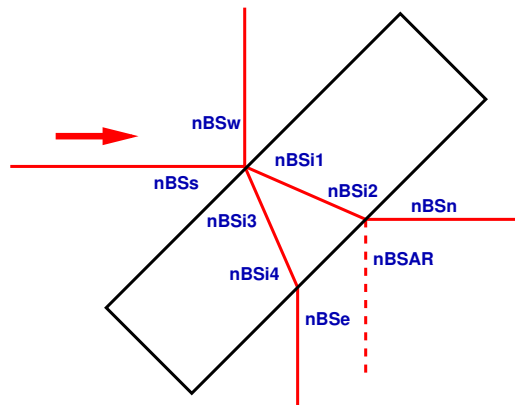


Figure 11: In FINESSE a beam splitter substrate is usually composed of three `bs` components and two spaces. This figures shows the node names for these components as used, for example, in file `05IB.kat`.

After leaving the IB the beam is passed though MPR and the main beam splitter (BS) before reaching the north arm cavity (file `05IB.kat`):

```

# power recycling mirror
m MPRo 0 1 0 nMPR1 nMPR2 # secondary surface, AR coated, curved
attr MPRo Rc -4.3 # nominal value
s sP 0.03 1.44963 nMPR2 nMPR3
m MP Ri 0 0.0783 0 nMPR3 nMPR4
s sS 5.96896 nMPR4 nBSs # distance PR-BS from OptoCad

# Beamsplitter, angles from OptoCad

```

```

bs BS 0.5025 0.49745 0 -44.978 nBSs nBSw nBSi1 nBSi3
s sBS1 0.0632 1.44963 nBSi1 nBSi2
s sBS2 0.0632 1.44963 nBSi3 nBSi4
bs BSAR1 0 1 0 -29.125 nBSi2 dump nBSn nBSAR
bs BSAR2 0 1 0 -29.125 nBSi4 dump nBSe dump

```

```
s sNs 6.19618 nBSn nMNI1 # distance BS-NI from OptoCad
```

The MPR has a curved secondary surface with an AR coating and thus serves as a lens. This lens, together with M_{IB5} and M_{IB6}, forms the mode matching telescope. The beam splitter is simply a cylindrical substrate, with the primary surface approximately $R = 50\%$ and a secondary surface with an anti-reflection coating (the residual reflection of approximately $R = 500$ ppm, not included in the simulation here). The two surfaces have an angle of 1.1 mrad with respect to each other.

A beam splitter in FINESSE looks rather complex since it must be entered as three `bs` components plus two spaces. This is due to the geometry of the beams inside the substrate (see Figure 11).

5.1 Beam size and shape

Unfortunately the beam size is not easy to measure at most locations inside the interferometer, because the beam is confined in a vacuum system. At the north end, the beam size could be measured relative to the cavity mode size by using a CCD camera. The CCD is located on the north terminal bench (B7p). The optics in front of the CCD are adjusted such that the camera is focused on the first lens after NE (L1). A Gaussian beam shape was fitted to the image of a the camera to obtain the beam size. It was not possible to get absolute numbers because the optical setup was not calibrated. Instead, the difference in size between the direct beam and the cavity mode were measured². The beam sizes were then calibrated by assuming that the cavity mode size is as expected. This is a reasonable approach since the cavity mode size would change little if the cavity mirrors had slightly wrong curvatures, whereas the beam size can change a lot for small deviations of the optics on the injection bench from their specifications.

The cavity mode size can be easily obtained by running `05IB.kat` with the command `trace 8` which prints the beam parameters at every node. We are interested in the beam parameters at the NI mirror and at the north end, here at L1, the lens after the NE mirror:

```

10: node nMNI1(31); MNIAR(3),sNs(30); n=1 (MNIAR --> nMNI1)
    x,y: w0=20.666266mm w=20.666266mm z=66.913626mm z_R=1.26105km
5: node nNB1(39); sN2(34),L1(36); n=1 (sN2 --> nNB1)
    x,y: w0=14.852735mm w=53.370079mm z=2.2480588km z_R=651.36008m

```

Thus we have the beam size of $w = 53.4$ mm at the lens after NE and $w = 20.7$ mm at NI for the eigen-mode of the north arm cavity. Using this number to calibrate the measurements we get the size of the direct beam as measured at L1: $w_x = 80.5$ mm, $w_y = 58$ mm for the horizontal and vertical size respectively.

After this measurement a mode matching of the beam to the north arm cavity has been performed. For this purpose the mode matching telescope on the IB was shortened (following the prediction of a FINESSE simulation). In total, the telescope length was reduced by approximately 4 mm and the input beam at the north end CCD became circular: $w_x = 61.5$ mm, $w_y = 60.6$ mm for the horizontal.

Using these values the input file `06matching` was created. It is based on `05IB` and was used to compute the power transmitted by the north cavity and the sizes of the input beam or the cavity mode the north end. The output of the simulation and the measured beam sizes are shown in Figure 12

Only a minimum number of parameters has been tuned to match the result to the measured values:

- Angle of incidence on M_{IB6} changed from 5° to 5.4° , to match the amount of astigmatism.

²The direct beam can be seen when the cavity is largely misaligned. The fact that the light power incident on the CCD is very different for the direct beam and the cavity mode can induce a measurement error due to nonlinearities of the CCD.

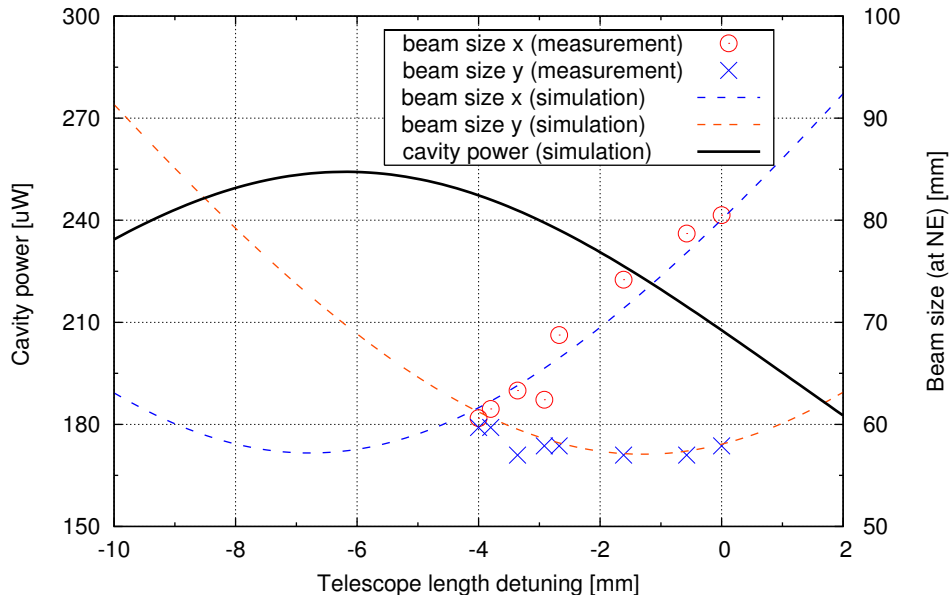


Figure 12: The power transmitted by the north cavity and the size of input beam measured at the north end (at the lens after NE). The data is plotted as a function of the mode matching telescope tuning, given as the change of the distance between M_IB5 and M_IB6. The measured beam sizes have been obtained during the so-called mode-matching activity when the telescope length was slowly reduced by 4 mm. (06matching.kat)

- Curvature of M_LIB6 was changed from 3.16 m to 3.138 m, to match the position of the minimum beam size as a function of the telescope tuning, see below.
- IMC waist size was changed from 5 mm to 4.26 mm to match the absolute size of the beams. This changes represents a relatively large deviation from the expected value and has to be investigated.

These changes are somewhat arbitrary, since similar results can also be achieved by other changes to the nominal parameters. But they represent one of the most likely combination of deviations.

The computations of the transmitted power and the beam sizes can both be done with 06matching.kat but have to be done separately. First we compute the beam sizes:

```
maxtem 0 # order of TEM modes (n+m)
bp wNE x w nNB1 # beam size at the lens L1 (horizontal)
bp wNE y w nNB1 # beam size at the lens L1 (vertical)
```

Since we only want to compute the propagation of the input beam through the optical system we do not need any higher order modes, hence we can use maxtem 0. The beam size in horizontal and vertical direction is plotted with the bp detector.

In all these examples with file 06matching.kat the length of the mode matching telescope is tuned by 12 mm: from an -10 mm to 2 mm offset with respect to the default length of 545 mm:

```
xaxis* s2 L lin -10m 2m 100 # tuning the distance between M_IB5 and M_IB6
# on the IB (i.e. the telescope length)
```

The power transmitted by the cavity has been measured before and after the beam matching and a 16% increase was found (again the absolute numbers itself are not meaningful, lacking a proper characterization of the optics in front of the diode B7). The transmitted power can be computed by FINESSE using the following commands in 06matching:

```

cav NC MNI nMNI2 MNE nMNE1      # compute cavity parameters
maxtem 4                          # order of TEM modes (n+m)
pd0 B7 noutB7                     # transmitted light power
trace 8                            # print beam parameters
    
```

The `cav` command ensures that the cavity is always on resonance³. As the mode mismatch in this example is quite large one should use a large number of modes; `maxtem 4` is probably too small for accurate results but it seems to be enough for qualitative results in this context (this can be checked by repeating the simulation with other settings for `maxtem`).

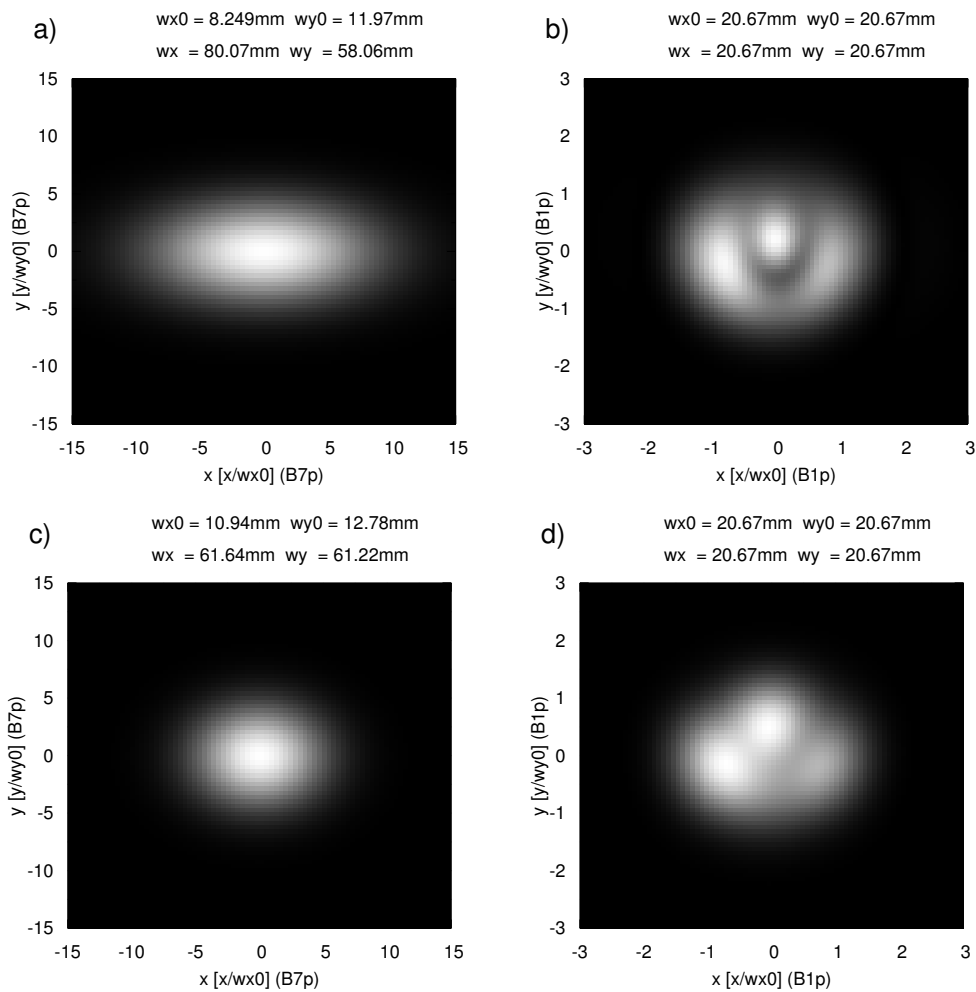


Figure 13: The shape of the beam before (top row) and after (bottom row) the mode matching activity. The plots in the left column, a) and c), show the beam as seen at L1, the lens after NE. The right plots, b) and d), show the shape of the beam reflected by the north cavity. Because of the mode matching the beam at the north end becomes more circular and the ring structure visible in the reflected light becomes less prominent. (07CCD.kat)

The graphical output of this simulation is shown in Figure 12 (together with the simulation and measurement of the beam sizes). The simulation gives $207 \mu\text{W}$ for the nominal telescope length, $247 \mu\text{W}$ for -4 mm detuning (i.e. the status after the beam matching) and $254 \mu\text{W}$ as the maximum that can be achieved by tuning that telescope length.

³ if a cavity is computed in a different base system than its eigen-modes the resonance condition of the cavity has (sometimes) to be carefully checked and set manually.

In addition, we can also quickly compute the transmitted power for a perfect mode matching of $272 \mu\text{W}$ by running `06matching.kat` again without explicitly setting a beam parameter for the input light:

```
l i1 6 0 0 nin
#gauss g1 i1 nin 4.26e-3 -42.836m # tuned to measured absolute beam size at NE
```

In this case the input beam is automatically matched to the cavity. We can see that by tuning only the telescope length, the best possible power that can be achieved is 93.4%. After the beam matching performed so far the power has reached 90.8% while before the beam matching we had only 76% of the maximum light power. Or in other words, by the beam matching performed so far the power should have increased by 18%.

Furthermore, FINESSE can be used to plot a ‘picture’ of the beam, as it would for example look like on a CCD camera. This feature can sometimes help to get a better intuitive understanding of the higher order modes. The shape of the input beam seen at the north end (passing a misaligned, unlocked cavity) can be plotted with (`07CCD.kat`):

```
# 1. beam shape of the input beam at the NE
# No ‘cav’ command, because cavity eigenmodes should not be used.
beam B7p nNB1
xaxis B7p x lin -15 15 80
x2axis B7p y lin -15 15 80
maxtem 0 # order of higher order modes (n+m)
```

In this example we only want to see the undisturbed input beam, so that only the lowest order mode must be used. If for example the shape of the beam reflected by the locked north arm cavity is to be plotted, one has to use many higher order modes because the beam shape will be dominated by the mode mismatch between the input light and the cavity eigen-mode. Figure 13 shows the beam shapes before and after the beam matching. The left column shows images of the input beam measured at the north end whereas the right column shows the shape of the beam reflected by the cavity.

6 Linear alignment

The control scheme for the linear alignment of VIRGO, and thus also of the north arm cavity has been designed and simulated but Gianfranco Giordano et.al. [5, 6]. The simulations shown here are a mere repetition of a smaller part of that work. As such they represent an easy task because the optical design is already known in advance. FINESSE is used here first as a tool for reverse engineering, i.e. to understand the properties of the optical setup as it was designed for VIRGO. Then the previously tuned input optics can be used to test if deviations of the optics will significantly change the linear alignment signals.

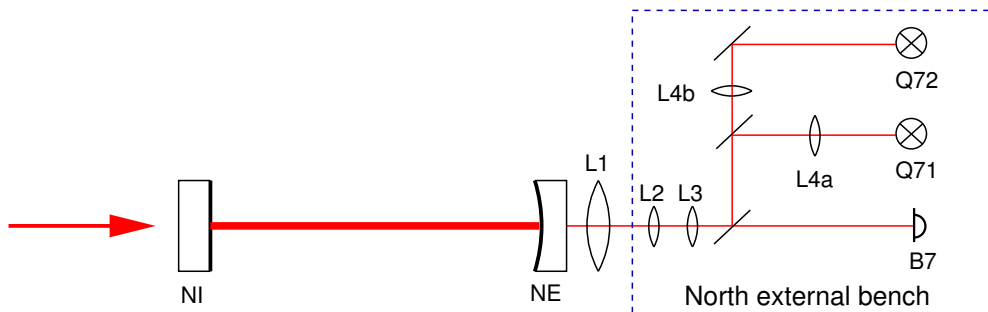


Figure 14: Simplified layout of the north external bench on which the photo diode B7 and the two quadrant diodes Q71 and Q72 are located.

The five lenses on the north terminal bench (see Figure 14) are used to achieve two goals: the Gouy phase of the beam between the NE mirror and the two quadrants should differ by exactly 90° and the beam size should be

reduced from more than 50 mm on the NE mirror to just a few millimeters so that quadrant diodes of standard size can be used for detection.

The full setup looks as follows (`08telescope.kat`):

```
# L1 first large lens after NE
s sN2 1.77 nMNE2 nL1
lens L1 1.02 nL1 nL2
# L2 and L3, small lenses after L1
s sN3 .8996 nL2 nL3
lens L2 -.2 nL3 nL4
s sN4 .2146 nL4 nL5
lens L3 -.1 nL5 nL6
s sN5 .365 nL6 nL7
# beam split into 50% going to B7 and 50% going to Q71, Q72
bs M71 .5 .5 0 0 nL7 nL8 nB7 dump
s sB7 0.97 nB7 noutB7
# beam split again 50/50, for Q71 and Q72
s sN6 .305 nL8 nL9
bs M72 .5 .5 0 0 nL9 nL10 nL11 dump
# lens L4a and Q71
s sN7 .10 nL10 nL12
lens L4a -.1 nL12 nL13
s sN8 .759 nL13 nQ71
# lens L4b Q72
s sN9 .286 nL11 nL15
lens L4b -.1 nL15 nL16
s sN10 .832 nL16 nQ72
```

To plot the Gouy phase that a beam will experience propagating through an optical system one can use the detector `gouy`. The beam size can again be plotted using `bp`. The output of `gouy` is in radian; here it is convenient to rescale this into degree:

```
# Plot Gouy phase from NE to quadrants on the north external bench
gouy gn1 x sN2 sN3 sN4 sN5 sN6 sN7 sN8
gouy gn2 x sN2 sN3 sN4 sN5 sN6 sN9 sN10

# Rescale Gouy phases from rad to degree
scale DEG gn1
scale DEG gn2

# Plot beam size at quadrants Q71 and Q72
bp w1 x w nQ71
bp w2 x w nQ72
```

In this case it makes sense to analyse the effect of a displacement of one lens (this example shows the effects of moving L2 because its positioning is the most critical one). In FINESSE one cannot directly tune the position of a lens. Instead the space components in front and behind the lens must be changed simultaneously (`08telescope.kat`):

```
xaxis* sN3 L lin -1m 1m 400
xparam sN4 L -1 1.1142
```

It turned out that the lens L1 currently installed induces a strong spherical aberration. The resulting distortion of the transmitted beam made it impossible to measure the beam parameters. This prevents a correct experimental tuning of the telescope. However, doing simulations like the one shown in Figure 15 is useful for understanding beforehand how the tuning can be performed.

When the Gouy phase is properly tuned one has to adjust the demodulation phase on the quadrant diodes to separate the signals, i.e. to obtain signals that are (for small angles) only proportional to a misalignment of one mirror while insensitive to the misalignment of the other. Figure 16 shows the response of Q71 and Q72 to a

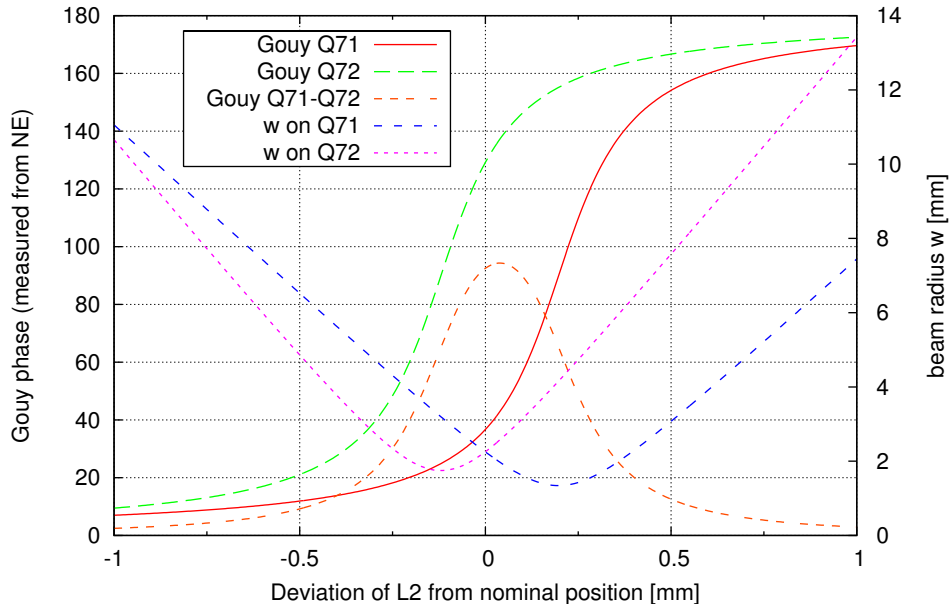


Figure 15: Tuning of the telescope on the north external bench. The plot shows the Gouy phase measured from NE to the quadrant diodes Q71 and Q72, the difference between these Gouy phases and the beam sizes on the two diodes. They are plotted as a function of the position of L2, the second lens after NE. The desired operating point is for a Guoy phase difference of 90° . Experimentally the tuning of L2 is difficult since it has to be positioned with an accuracy of ± 1 mm. A good measure is the size of the beam on the quadrants: at the operating point the beam sizes should be equal. (08telescope.kat)

misalignment of the NE mirror after the demodulation phase has been tuned so that Q71 is mostly insensitive to the NE angular position. For simplicity, in this simulation (09ne-signal.kat) the input beam is replaced by a dummy input (as in file 04modulation.kat and before) so that the astigmatism and mode-mismatch is not taken into account. In order to plot the signals for horizontal alignment, the following commands are used:

```
pd1 Q71 $fMI -10 nQ71
pdtype Q71 x-split
pd1 Q72 $fMI -3 nQ72
pdtype Q72 x-split
```

```
xaxis MNE xbeta lin -10u 10u 200
```

```
cav NC MNI nMNI2 MNE nMNE1      # compute cavity
maxtem 4                          # order of higher order modes (n+m)
```

The modal expansion requires in principle many more modes than specified by `maxtem 4` to compute correct results for angles up to $10 \mu\text{rad}$. Increasing this number will change the outer wings of the error signal, as shown in Figure 16. Please be aware of the fact that even with a large number of higher order modes the results cannot represent the real error signals because in this simulation the longitudinal deviation from the operating point induced by the misalignment is not compensated.

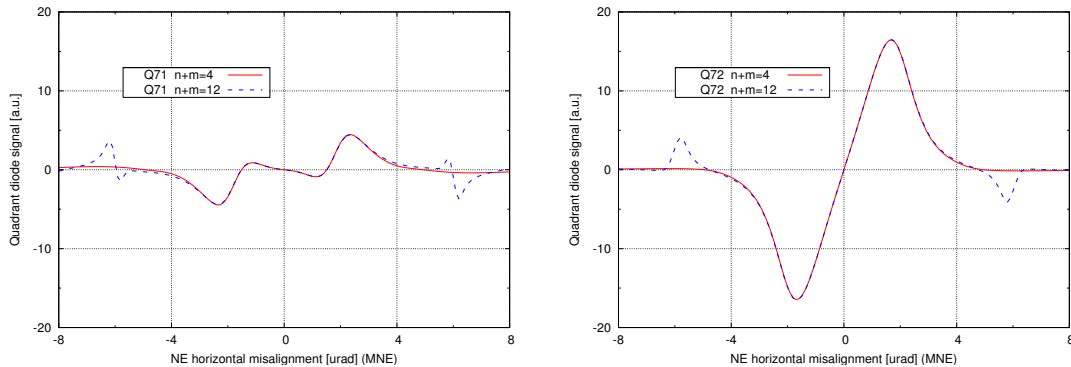


Figure 16: The error signal from the two quadrant diodes Q71 and Q72. The simulation has been done with `maxtem 4` and `maxtem 12` in order to demonstrate that for larger angles many higher order modes must be used whereas the signal slope around zero is computed correctly with less modes. Please note that the deviation from the longitudinal operating point induced by the misalignment is not compensated in this simulation so that the experimental setup is not yet correctly reproduced. (`09ne-signal.kat`)

7 Conclusion

We have created an input file for the interferometer simulation software FINESSE that holds all the optical components for the north arm of the VIRGO detector, starting at the output mirror of the IMC, up to the quadrant diodes on the north external bench. The simulation has been used to support the experimental work on:

- the optical setup on the north external bench
- the optical characterisation of the north arm cavity
- the characterisation of the modulation frequency
- the implementation of the linear alignment control
- the mode matching of the input beam to the arm cavities

During this work the parameters of the file have been adjusted in accordance with measurements. The input file has been tuned to reproduce measured data and can be considered as a good description of the optical setup as it exists today. The following parameters were adjusted:

- Radius of curvature of NE from 3600 m to 3530 m
- Finesse of north arm cavity from 50 to 43 by arbitrarily reducing the reflection of NI (this value has to be understood as ‘between 50 and 40’ since its tuning was not done accurately)
- Waist size of IMC from 4.9 mm to 4.3 mm
- Angles of incidence of M_IB5 and M_IB6 and radius of curvature of M_IB6 have been adjusted only slightly.

In the following these files will be used to create an input file for full VIRGO detector that allows to compute, for example, locking signals, linear-alignment signals, noise couplings and of course the power and shape of the various beams.

References

- [1] C. Bradaschia *et al.*, *Nuclear Instruments and Methods in Physics Research A* **289**, 518–525 (1990). 1

- [2] A. Freise, G. Heinzl, H. Lück, R. Schilling, B. Willke and K. Danzmann: ‘Frequency domain interferometer simulation with higher-order spatial modes’, *Class. Quantum Grav.* **21** (2003).
The program is currently available at <http://www.rzg.mpg.de/~adf> **1**
- [3] A. Freise : the FINESSE input files noted in this document, 2004,
<http://wwwcascina.virgo.infn.it/alignment/simulation/finesse/files/northarm>. **1**
- [4] R. Schilling: ‘OPTOCAD, A Fortran 95 module for tracing Gaussian beams through an optical set-up, Version 0.74’, internal note, 2002. **12**
- [5] D. Babusci, H. Fang, G. Giordano, G. Matone, V. Sannibale, *Phys. Lett. A* **226**, 394 (1997). **17**
- [6] G. Giordano et. al. <http://www.lnf.infn.it/esperimenti/virgo/linear> **17**
- [7] D. Z. Anderson, “Alignment of resonant optical cavities”, *Appl. Opt.* **23** 2944–2949 (1984). **7**